Scripta Materialia 155 (2018) 99–103

Contents lists available at ScienceDirect

Scripta Materialia

journal homepage: www.elsevier.com/locate/scriptamat

Regular article

Vanishing of room-temperature slip avalanches in a face-centered-cubic high-entropy alloy by ultrafine grain formation

Jian Qiang [a,*], Koichi Tsuchiya [a,b,*], Haoyan Diao [c], Peter K. Liaw [c]

[a] National Institute for Materials Science, 1-2-1 Sengen, Tsukuba, Ibaraki 305-0047, Japan
[b] University of Tsukuba, 1-1-1 Tennodai, Tsukuba, Ibaraki 305-8577, Japan
[c] The University of Tennessee, Knoxville, TN 37996, USA

ARTICLE INFO

Article history:
Received 15 May 2018
Received in revised form 13 June 2018
Accepted 13 June 2018
Available online xxxx

Keywords:
High-entropy alloy
High-pressure torsion
Hardness test
Nanoindentation
Slip

ABSTRACT

High-pressure torsion (HPT) was applied to $Al_{0.3}$CrFeCoNi high-entropy alloy to study the effect of severe grain-refinement on the deformation behavior. After 10 rotations of HPT, the grain size was reduced to tens of nanometers. Nano-twins and stacking faults were found in the nano-grained samples. This nano-grain formation led to an obvious increase in micro-Vickers hardness, and vanishing of slip avalanches during nanoindentation which was evidenced by the absence of pop-ins in the loading segment. These phenomena can be attributed to the affluent grain boundaries that acted as extra mediators for plastic deformation and obstacles for the propagation of lattice dislocations.

High-entropy alloys (HEAs) are composed of multiple elements at an equiatomic or near equiatomic ratio. The random mixing of the constituent elements significantly increases the configurational entropy of mixing, leading to an effectively-low Gibbs free energy of mixing [1–16]. Consequently, some HEAs can be solidified into single-phase solid-solutions with simple lattice structures, such as face-centered cubic (fcc) [2–4, 7, 9, 10, 12–18] or body-centered cubic (bcc) [4, 5, 7, 8, 10–12, 14–16, 19, 20], instead of intermetallic compounds. On the other hand, recent studies also suggest that the random mixing has a significant influence on the properties of HEAs. Zhang et al. found that increasing chemical disordering and lattice distortion can enhance electron and phonon scattering, which explained why NiCoFeCr exhibited larger thermal and electrical resistivity than Ni, NiFe, and NiCo [21]. Carroll et al. reported that serrations can be observed in the stress-strain curves for CoCrFeMnNi, CoCrFeNi, and CoFeNi alloys in certain temperature windows; whereas no such behavior can be seen for NiCo or Ni [22]. Additionally, Yasuda et al. proposed that the addition of Al could facilitate the generation of serration as Al atoms increase the friction of dislocations [23].

Besides in HEAs, serration has also been documented in various metallic materials, including steels [16, 24, 25], Al alloy [16, 26] and even metallic glasses [16, 27–29]. It is believed that what phenomenally appears as serration is caused by slip avalanches, which is related to the escape and arrest of the shear deformation in a small volume in the material [30]. The shear can be attained either by dislocation slip (in crystalline materials) or by shear transformation zone (in metallic glass). It has been confirmed that temperature, strain rate [22, 31] and even fabrication method [32] could significantly affect the serration behavior. However, little is known about the influence of grain boundary. Given that many metals and alloys in structural applications are polycrystalline and that grain boundary can act as an obstacle for dislocation movement as well as a source for dislocation, the role of the grain boundary is worth studying.

The constituent phases of the Al-containing HEA system Al_xCrFeCoNi have been studied extensively. It is reported that a low Al concentration ($x = 0.3$) facilitated the formation of fcc phase, whereas a high Al ratio ($x = 0.5$ and 0.7) could lead to the formation of bcc phases [33]. In this letter, we report room-temperature slip avalanches manifested as multiple pop-ins in the nanoindentation load-depth curve for the coarse-grained $Al_{0.3}$CrFeCoNi (atomic ratio) HEA, which is different from the cases observed in conventional compression or tensile tests where elevated-temperatures are necessary [22, 23, 31, 34, 35]. As a comparison, nanoindentation is also performed on the nanocrystalline sample after grain-refinement by the high-pressure torsion (HPT) technique. The evolution of the mechanical property and the deformation behavior was investigated.

Cylindrical $Al_{0.3}$CrFeCoNi HEA samples in a diameter of 7 mm were prepared by the tilt-casting method. The as-cast rods were sliced into disks before being subjected to HPT deformation. HPT deformation

* Corresponding authors at: National Institute for Materials Science, 1-2-1 Sengen, Tsukuba, Ibaraki 305-0047, Japan.
E-mail addresses: QIANG.Jian@nims.go.jp, (J. Qiang), TSUCHIYA.Koichi@nims.go.jp (K. Tsuchiya).

https://doi.org/10.1016/j.scriptamat.2018.06.034
1359-6462/

was conducted under a compressive pressure of 10 GPa at room temperature at a rotation speed of 1 rpm for various numbers of rotations ($N = 1$, 3, and 10). The microstructure of the as-cast sample was confirmed by electron backscattered diffraction (EBSD) using a Zeiss-Sigma field-emission scanning electron microscope (SEM) operated at 20 kV. The phase compositions of the as-cast and deformed samples were identified using X-ray diffraction (XRD, Rigaku TTR III) with Cu-K_α radiation, which was performed on the samples mechanically ground to the median plane. The microstructure of the sample deformed by 10 rotations was also examined by JEOL JEM-2100 and 2010F transmission electron microscopes (TEMs) with an accelerating voltage of 200 kV. The mechanical properties were analyzed by micro-Vickers hardness and nanoindentation tests. The former was measured employing a Matsuzawa MMT-X on the cross-section with an applied load of 200 gf and period of 15 s. Nanoindentation was performed using a Hysitron Triboindenter TI950 with a Berkovich indenter under a load-control mode at a loading rate of 250 μN/s. At least 15 indents were performed on each sample.

It was confirmed by XRD measurements that the sample has a single-phase fcc structure with a lattice parameter of 0.360 nm, and remained so after 1, 3 and 10 rotations of HPT deformation (Supplementary data Fig. S1). The as-cast sample was composed of coarse grains with the sizes of hundreds of microns (Supplementary data Fig. S2). The application of HPT deformation on the as-cast sample caused considerable grain refinement. Fig. 1(a) shows the backscattered electron (BSE) SEM image of the center part of the sample deformed by 1 rotation. Fragmentation of the original grains into submicron grains and the formation of nanoscale shear bands nearly parallel to the shear planes can be seen. At the periphery of the disk (not shown), the grains were further reduced to smaller sizes than the center part of the disk. The bright-field TEM images in Fig. 1(b) shows that after 10 rotations the average grain size has decreased to tens of nanometers. Besides, some of the grain boundaries are not clearly seen due to the severe lattice distortion, suggesting slow dynamic recovery and recrystallization. The Debye-Scherer ring pattern in the selected-area diffraction shown as the inset of Fig. 1(b) is typical for a polycrystalline fcc in accordance with the XRD results. Fig. 1(c) is a high-resolution TEM image of grains in the sample after 10 rotations. Several line features are seen within the nano-grains. They are nanotwins or stacking faults as seen in the inset. It is worth mentioning that although twinning has been often observed for the CrMnFeCoNi HEA deformed at cryogenic temperatures [17], it is more difficult for the twinning to happen for this Al-containing HEA due to a much higher stacking fault energy (SFE) than in CrMnFeCoNi [23]. The present results indicate that even for the alloys with higher SFE nanotwin can be activated due to enhanced activity of Shockley partial dislocations as was observed in nano-grained aluminum [36].

The change in the microstructure led to pronounced strain-hardening. Micro-Vickers hardness measured on the cross-section of the as-cast and HPT-deformed samples are plotted as a function of the distance from the center in Fig. 2(a). The hardness in the as-cast state was 156 ± 5 H_v. HPT deformation led to a drastic increase in the hardness. For the sample deformed by 1 rotation, the hardness slightly increased with the distance from the center, and the maximum of 493 ± 6 H_v was obtained at the position 3 mm from the center. A similar tendency was also observed for the sample deformed by 3 rotations, except that the hardness seemed to saturate before reaching the sample periphery. The difference in hardness along the radial distance can no longer be seen for the sample deformed by 10 rotations, indicating the microstructure became more homogeneous at this strain level. Fig. 2(b) is the BSE image showing the morphology of the indent for the as-cast sample. Slip traces, i.e. the intersection of the slip plane and the sample surface produced by gliding dislocations, appeared around the indent. Specifically at the top left side, two slip systems seemed to have activated, as evidenced by two sets of parallel yet intersecting lines. The detail of the slip traces can be seen from the inset of Fig. 2(b).

Nanoindentation was also performed to reveal the change in nanomechanical behavior. Fig. 3(a) shows the representative load-depth curves obtained from: the as-cast sample, the center of the sample deformed by 1 rotation, and the edge of the sample (3 mm from the center) deformed by 10 rotations. These samples and positions were chosen according to their respective micro-Vickers hardness. It is clear that the loading part for the as-cast sample exhibited multiple pop-ins, whereas the curves were quite smooth for the other two samples deformed by HPT. Molecular dynamics simulations conducted on single crystal fcc metals proposed that a pop-in event was related to the collective nucleation of dislocations beneath the indent [37, 38]. Unlike metals or alloys with a bcc lattice structure displaying one pronounced pop-in [39, 40], this HEA showed multiple smaller pop-ins. The results obtained from single crystal Mo (bcc) and Ni (fcc) seemed to suggest that the difference in the magnitude and number of pop-in can be attributed to different dislocation-nucleation processes: perfect dislocations in bcc crystals and partial dislocations in fcc crystals [40]. Fig. 3(b) shows the

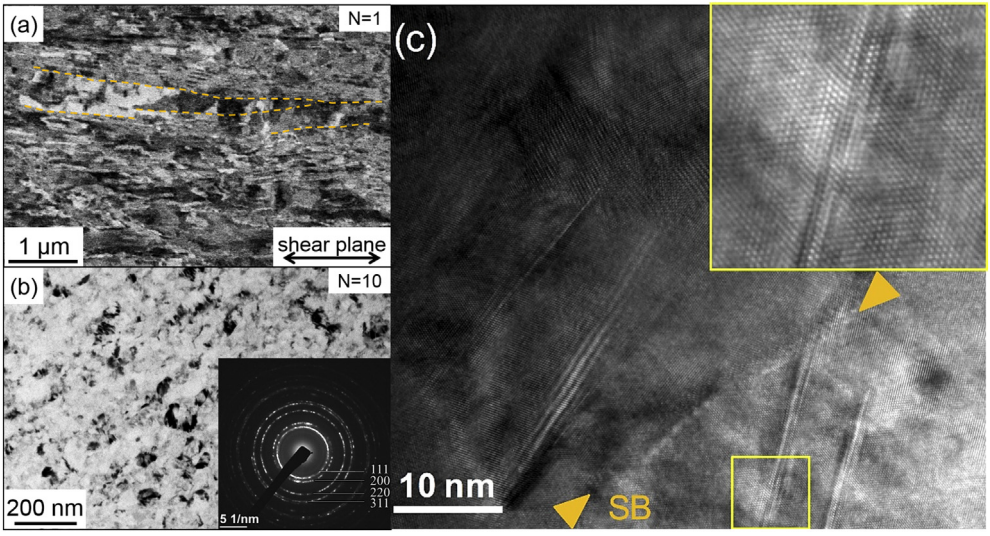

Fig. 1. (a) BSE-SEM image for the center of the sample deformed by 1 rotation. Some shear bands are highlighted by the dash lines. (b) Bright-field TEM image for the sample deformed by 10 rotations. The inset is the selected area diffraction pattern. (c) High-resolution TEM image of the sample deformed by 10 rotations. The inset is an enlarged view of the boxed area. SB: sub-boundary.